

## High-throughput assembly of nanoelements in nanoporous alumina templates

Evin Gultepe, Dattatri Nagesha, and Latika Menon

*Electronics Materials Research Institute, Northeastern University, Boston, Massachusetts 02115 and  
Department of Physics, Northeastern University, Boston, Massachusetts 02115*

Ahmed Busnaina

*Center for High Rate Nanomanufacturing, Northeastern University, Boston, Massachusetts 02115 and  
Department of Mechanical and Industrial Engineering, Northeastern University, Boston, Massachusetts 02115*

Srinivas Sridhar<sup>a)</sup>

*Electronics Materials Research Institute, Northeastern University, Boston, Massachusetts 02115 and  
Department of Physics, Northeastern University, Boston, Massachusetts 02115*

(Received 7 February 2007; accepted 22 March 2007; published online 20 April 2007)

The authors demonstrate a nanofabrication method utilizing nanoporous alumina templates which involves directed three dimensional assembly of nanoparticles inside the pores by means of an electrophoretic technique. In their demonstration, they have assembled polystyrene nanobeads with diameter of 50 nm inside nanopore arrays of height of 250 nm and diameter of 80 nm. Such a technique is particularly useful for large-scale, rapid assembly of nanoelements for potential device applications. © 2007 American Institute of Physics. [DOI: [10.1063/1.2730575](https://doi.org/10.1063/1.2730575)]

Nanomaterials in the form of nanoparticles, nanowires, and nanotubes are the main components in the burgeoning field of nanotechnology. Due to their unique physical and chemical properties, these nanoelements have the potential for use in a variety of applications such as memory devices,<sup>1</sup> chemical sensors,<sup>2</sup> biosensors,<sup>3,4</sup> in diagnostics,<sup>5</sup> and imaging.<sup>6</sup> However, an important challenge in nanomanufacturing is the directed growth or assembly of nanoelements over macroscopic length scales. Different strategies have been explored to address the two dimensional (2D) and three dimensional (3D) assemblies of nanomaterials. Using capillary forces, spherical colloidal particles (>150 nm) have been assembled in microfabricated patterns of various shapes.<sup>7</sup> Sub-50 nm colloids were assembled on a lithographically patterned surface by a mechanism known as capillary force assembly.<sup>8</sup> Another approach involves bias induced assembly. For example, CdS colloids have been assembled within the trenches created on block copolymers by application of bias voltage.<sup>9</sup> Very recently, a similar approach utilizing electric field assisted oriented assembly of CdS nanorods has also been demonstrated.<sup>10</sup> Biological elements in the form of DNA,<sup>11</sup> bacteria,<sup>12</sup> and viruses<sup>13</sup> have also been used as templates for assembly of nanoscale elements. These techniques all have limitations for assembly of nanoelements on large centimeter scales or for rapid assembly and utilize expensive and time consuming processes. Assembly of nanoparticles into macroscopic structures that have all dimensions in the nanometer length scale is still quite a formidable challenge.

In this letter we report a different kind of nanoassembly technique utilizing nanoporous alumina templates. Charged nanoparticles in solution are assembled inside the pores by means of an electrophoretic process. This method is the demonstration of directed assembly in truly 2D nanostructures. It also demonstrates a very simple technique for rapid and large-scale assembly of nanoelements.

Ordered nanoporous alumina templates were prepared by anodization of aluminum foil in an acid solution. For this, a commercially available Al foil was used as anode, graphite sheet was used as cathode, and 5 wt % oxalic acid as the electrolyte. Anodization was carried out at 4 °C for 6 h under a constant of 50 V direct current (dc) potential. This produced a thick layer (~tens of microns) of porous aluminum oxide consisting of an array of vertically arranged pores on the surface of aluminum. The thick porous layer was then completely removed by soaking in chromic-phosphoric acid solution for about 20 h, which leaves behind a highly ordered patterned Al surface. The patterned aluminum surface was then reintroduced in the acid bath for a second anodization under the same experimental conditions for around 5 min. This second step produced a periodic, hexagonally ordered nanoporous layer with pore diameter of the order of 30 nm and thickness of the order of 500 nm.

The porous layer is separated from the bottom conducting aluminum layer by a thin layer of barrier aluminum oxide. For efficient electrophoretic assembly, an important requirement is the presence of a conducting surface below the pores. It is therefore important to etch the barrier layer below the pores. For this, the sample was soaked in 5% phosphoric acid for about 80 min. This results in thinning of the barrier layer at the bottom of the nanoholes. Additionally, this leads to widening of the pore diameter of individual nanopores and decrease in the height of the nanoporous film. A representative scanning electron microscope (SEM) image is shown in Fig. 1. Typical pore diameter of the templates is in the order of 75–80 nm [Fig. 1(a)] and thickness of the order of 250 nm [Fig. 1(b)]. Such templates were used for the assembly of nanobeads, as discussed below.

Electrophoresis involves the motion of colloidal particles in solution in an applied electric field. In this work, we have demonstrated this technique for the assembly of nanobeads within the nanoporous alumina template. In the case of colloidal particles, when such particles are in contact with a liquid, a thin layer (the so-called electrical double layer) with

<sup>a)</sup>Electronic mail: s.sridhar@neu.edu

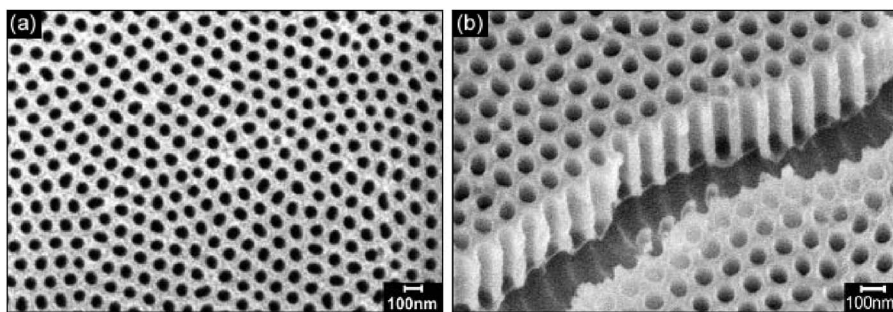


FIG. 1. SEM images of nanoporous alumina nanotemplate. (a) Plan view image of template with uniform periodic nanoholes over large length scales, scale bar=100 nm and (b) cross-section view of the template showing smooth cylindrical nanochannels about 250 nm in height extending to the bottom of the aluminum substrate, scale bar=100 nm.

a nonzero net charge density is produced by rearrangement of local free ions in the solution. For spherical particles, the relation between the velocity ( $\mathbf{v}$ ) of the particles and the electric field ( $\mathbf{E}$ ) is given by  $\mathbf{v} = \mu_e \mathbf{E}$ , where,  $\mu_e$  is the electrophoretic mobility.<sup>14</sup> For a spherical particle in a liquid, electrophoretic mobility is calculated as  $\mu_e = (2\varepsilon\zeta/3\eta)f_1(\kappa a)$ , where  $\varepsilon$  is dielectric constant of the liquid,  $\zeta$  is zeta potential of the particle in the solution,  $\eta$  is viscosity of the liquid, and  $\kappa$  is Debye-Hückel parameter which depends only on temperature and the bulk electrolyte concentration.  $f_1(\kappa a)$  is monochromatically varying function in the range of  $1.0(\kappa a=0) - 1.5(\kappa a=\infty)$ .<sup>15</sup> The well-known Smoluchowski equation ( $\mu_e = \varepsilon\zeta/\eta$ ) is the upper limit of this equation. Using the Smoluchowski equation and equation  $\mathbf{v} = \mu_e \mathbf{E}$ , the speed of the beads during assembly was calculated to be approximately 1 mm/min, where the potential difference between the electrodes is 10 V, the  $\zeta$  potential of the beads is  $-40$  mV, and the dielectric constant and the viscosities of the water are taken as 80.1 and 0.89 mPa s respectively.<sup>16</sup> It must be noted that other parameters such as high applied voltage, interparticle, or particle-wall interactions can also affect the electrophoresis,<sup>17</sup> however, the above calculations give a basic estimate for the required experimental parameters.

For assembly of 50 nm polystyrene latex beads within nanoporous alumina templates, an electrolyte consisting of the nanobeads mixed in ethanol (5  $\mu\text{l/ml}$  concentration) was used. Electrical contact was made to the conducting aluminum layer below the alumina template and was maintained at 10 V value with respect to the counterelectrode which was grounded. Template was placed in the holder which allows electrical contact at the bottom and then it was filled with 50  $\mu\text{l}$  of electrolyte so that alumina template was completely submerged. As a counterelectrode, a Pt-Ir wire was brought close to the template surface, at a distance of  $\sim 50$   $\mu\text{m}$  from template for a time duration of around 2 min. Schematic illustration of the experimental setup is shown in Fig. 2. At a dc bias of 10 V, the negatively charged polystyrene nanobeads are found to assemble inside the pores over 10  $\mu\text{m}$  diameter region around the counterelectrode wire. This region corresponds to the region over which the bias is applied. Figures 3(a) and 3(b) are representative SEM images of nanobead assembly within nanoporous alumina template. The low resolution SEM shows that assembly only occurred in areas that are in close proximity to the counterelectrode and not in other areas on the template surface. The complete assembly was confirmed by the cross-section SEM image [Fig. 3(b)] which shows 100% assembly: all of the holes are completely filled by nanobeads. Thus by varying the size and height of the nanohole, the number of beads assembled can be manipulated.

Theoretical modeling has been used to predict the electrical field distribution within the nanoporous alumina array during the electrophoresis process. The effect of the thickness of the insulating alumina layer (barrier layer) at the bottom of the nanoholes, film thickness, and type of electrolyte on the electrical field distribution was studied. Distribution of electric fields inside the nanopores due to the applied voltage was studied by means of the simulation program ANSYS (ANSYS, Inc., Canonsburg, PA). A simplified model for porous alumina was assumed with 16 nanoholes, 250 units in thickness, with 10 units in barrier layer, and 80 units in diameter—conditions similar to the experimental parameters. The medium between the electrodes and inside the alumina holes is assumed to be water. The dielectric constants of alumina and that of the electrolyte were approximated to be around 9 and 80, respectively.<sup>16</sup> Similar to experimental conditions, 10 V dc bias was applied between the electrodes for modeling calculations.

The construction of the model is shown in Fig. 4(a), representing the positive electrode inside the alumina layer with nanoholes. The color scale in the diagram indicates the variation in the magnitude of the electric field in arbitrary units. Figures 4(b) and 4(c) show the longitudinal and perpendicular cross-section images of electric field distribution. Thus even in the presence of the insulating barrier layer, the strong electric field is directed towards the center of the

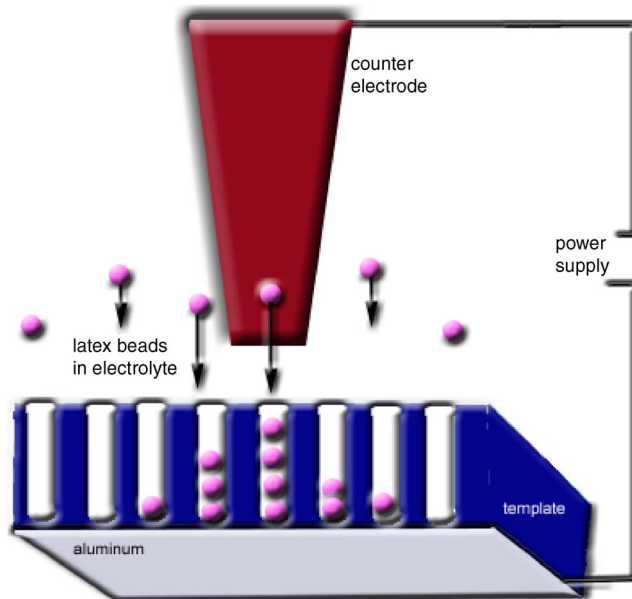


FIG. 2. (Color online) Schematic illustration of electrophoresis experiment setup. The arrows represent the velocity of the beads by the electrophoretic force.

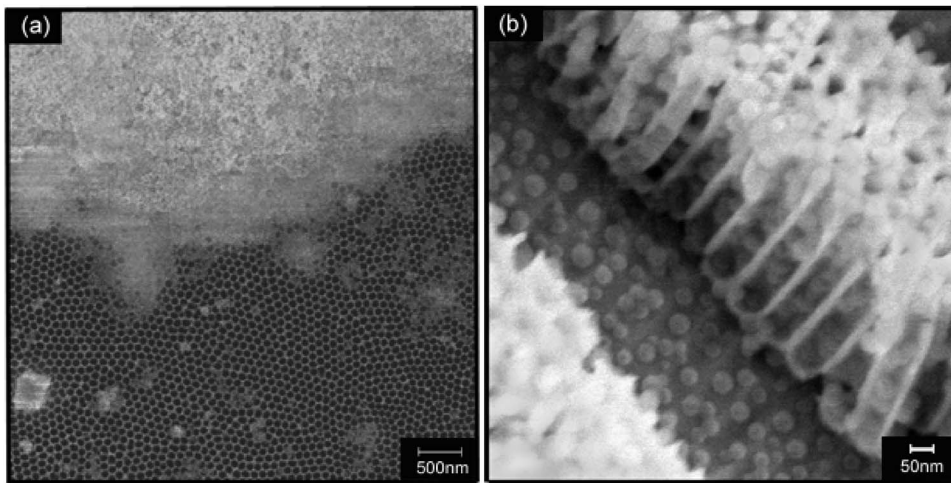


FIG. 3. SEM images of nanobeads assembly in nanoporous alumina nanoarray. (a) Assembly occurs where the counterelectrode gets close, not the other parts of template. (b) 100% assembly of loaded nanobeads.

nanoholes so that charged particles are attracted into the holes.

In conclusion, we have demonstrated 3D assembly of polymer nanobeads inside nanoholes in porous alumina. This

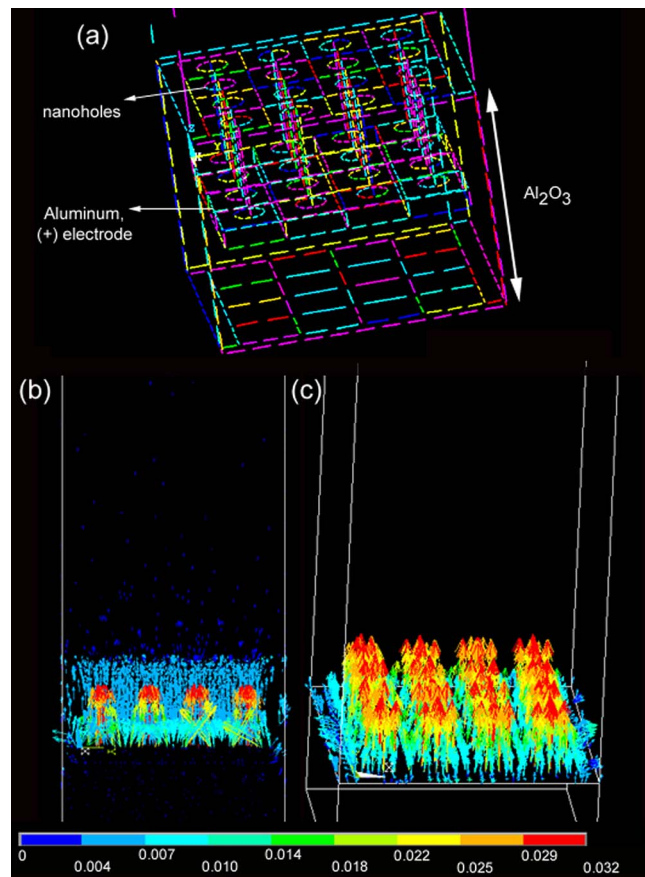


FIG. 4. (Color online) Theoretical modeling for electric field distribution during electrophoretic assembly by ANSYS. (a) Configuration of positive electrode representing nanoholes, alumina nanoarrays, and aluminum electrode. (b) Longitudinal cross section of electric field distribution shows that electric field magnitude increases (brighter red arrows) inside the nanoholes. (c) A perpendicular cross section shows that at the template boundary there is a considerable difference in electric field magnitude between the holes (red arrows) and the surface (blue arrows). The length of arrows is proportional to the magnitude of the vector and color scale is in arbitrary units.

work demonstrated that reliable approaches to nanoassembly are feasible and forms the basis for a variety of other nanoassembly challenges. For example, drug-loaded polymeric nanoparticles could be assembled with these nanoporous arrays and used as drug delivery platform. Another possible application for these nanoporous arrays is in the vertical assembly of single walled carbon nanotubes (SWCNTs) within the nanoporous array. Vertically aligned SWCNTs have the potential for use as vertical interconnects in carbon nanotube-based integrated circuit chips.

This work was supported by the National Science Foundation (NSF) Nanoscale Science and Engineering Centers Program (NSF-0425826) and the IGERT Nanomedicine Science and Technology Program (NSF-0504331).

- <sup>1</sup>T. Rueckes, K. Kim, E. Joselevich, G. Y. Tseng, C. L. Cheung, and C. M. Lieber, *Science* **289**, 94 (2000).
- <sup>2</sup>Y. Cui, Q. Wei, H. Park, and C. M. Lieber, *Science* **293**, 1289 (2001).
- <sup>3</sup>W. U. Wang, C. Chen, K.-H. Lin, Y. Fang, and C. M. Lieber, *Proc. Natl. Acad. Sci. U.S.A.* **102**, 3208 (2005).
- <sup>4</sup>D. G. Georganopoulou, L. Chang, J.-M. Nam, C. S. Thaxton, E. J. Mufson, W. L. Klein, and C. A. Mirkin, *Proc. Natl. Acad. Sci. U.S.A.* **102**, 2263 (2005).
- <sup>5</sup>J.-M. Nam, C. S. Thaxton, and C. A. Mirkin, *Science* **301**, 1884 (2003).
- <sup>6</sup>J. L. West and N. J. Halas, *Curr. Opin. Biotechnol.* **11**, 215 (2000); S. K. Sahoo and V. Labhasetwar, *Drug Discovery Today* **8**, 1112 (2003).
- <sup>7</sup>Y. Yin, Y. Lu, B. Gates, and Y. Xia, *J. Am. Chem. Soc.* **123**, 8718 (2001).
- <sup>8</sup>Y. Cui, M. T. Bjork, J. A. Liddle, C. Sonnichsen, B. Boussert, and P. A. Alivisatos, *Nano Lett.* **4**, 1093 (2004).
- <sup>9</sup>Q. Zhang, T. Xu, D. Butterfield, M. J. Misner, D. Y. Ryu, T. Emrick, and T. P. Russell, *Nano Lett.* **5**, 357 (2005).
- <sup>10</sup>K. M. Ryan, A. Mastroianni, K. A. Stancil, H. Liu, and A. P. Alivisatos, *Nano Lett.* **6**, 1479 (2006).
- <sup>11</sup>K. Bandyopadhyay, E. Tan, L. Ho, S. Bundick, S. M. Baker, and A. Niemz, *Langmuir* **22**, 4978 (2006).
- <sup>12</sup>V. Berry and R. F. Saraf, *Angew. Chem., Int. Ed.* **44**, 6668 (2005).
- <sup>13</sup>K. T. Nam, D.-W. Kim, P. J. Yoo, C.-Y. Chiang, N. Meethong, P. T. Hammond, Y.-M. Chiang, and A. M. Belcher, *Science* **312**, 885 (2006).
- <sup>14</sup>R. J. Hunter, *Foundations of Colloid Science* (Oxford University Press, New York, 2001), pp. 380–384.
- <sup>15</sup>D. C. Henry, *Proc. R. Soc., London* **133**, 106 (1931).
- <sup>16</sup>D. R. Lide, *CRC Handbook of Chemistry and Physics*, 76th ed. (CRC, Boca Raton, FL, 1995), pp. 6–160.
- <sup>17</sup>Robert J. Hunter, *Foundations of Colloid Science* (Oxford University Press, New York, 2001), pp. 393–395.